Superconductivity in AuNiGe ohmic contacts to a GaAs-based high mobility two-dimensional electron gas

C. B. Beauchamp,[1] S. Dimitriadis,[1] J. T. Nicholls,[1, a)] L. V. Levitin,[1] A. J. Casey,[1] P. See,[2] G. Creeth,[3] J. Waldie,[4] I. Farrer,[4, 5] H. E. Beere,[4] and D. A. Ritchie[4]

[1)] *Physics Department, Royal Holloway, University of London, Egham TW20 0EX, United Kingdom*
[2)] *National Physical Laboratory, Hampton Road, Teddington, Middlesex, TW11 0LW, United Kingdom*
[3)] *London Centre for Nanotechnology, University College London, 17-19 Gordon Street, London WC1H 0AH, United Kingdom*
[4)] *Cavendish Laboratory, University of Cambridge, JJ Thomson Avenue, Cambridge, CB3 0HE, United Kingdom*
[5)] *Department of Electronic and Electrical Engineering, University of Sheffield, Mappin Street, Sheffield S1 3JD, United Kingdom*

(Dated: 6 October 2020)

To cool a high mobility two-dimensional electron gas (2DEG) at a GaAs-AlGaAs heterojunction to milliKelvin temperatures, we have fabricated low resistance ohmic contacts based on alloys of Au, Ni and Ge. The ohmic contacts have a typical contact resistance of $R_C \approx 0.8\ \Omega$ at 4.2 K, which drops to 0.2 Ω below 0.9 K. Scanning electron microscope images establish that the contacts have the same inhomogeneous microstructure that has been observed in previous studies. Measurements of the contact resistance R_C, the four-terminal resistance along the top of a single contact, and the vertical resistance R_V, all show that there is a superconductor in the ohmic contact which can be turned completely normal with a magnetic field of 0.15 T. We briefly discuss how this superconductivity may be affecting the electrical transport measurements of 2DEGs, especially how it may hinder the cooling of electrons in a 2DEG below 0.1 K.

In the long-standing quest to discover new many-body states in low-dimensional electron systems, it is desirable to cool two-dimensional electron gas (2DEG) devices to the lowest possible temperatures. At low T the lattice and electrons thermally decouple, and if there is a heat leak to the electrons they heat up to a temperature T_e that is higher than the lattice temperature T_L. Much experimental effort, for example, filtering the electrical leads and shielding the sample from radiation, has been made to reduce the heat leak, and the lowest confirmed 2DEG temperature is $T_e = 6$ mK by Iftikar *et al.*[1] measured using three in situ primary thermometers. The ability to cool low-dimensional electrons below 10 mK has allowed studies of Tomonaga-Luttinger liquids[2] and the multichannel Kondo effect.[3]

Insight into how the electrons are cooled is obtained by Joule heating the electron gas with a power P, the electrons thermalize at a temperature T_e and the rate at which they lose their excess energy to the lattice at T_L is expressed as $P = \dot{Q}(T_e) - \dot{Q}(T_L)$. Experimentally it was found[4] that $\dot{Q}(T) = aT^5 + bT^2$, where the T^5 term is electron-phonon cooling and the T^2 is cooling via the ohmic contacts. At high temperatures the T^5 term dominates, whereas below 100 mK the electrons are predominantly cooled through the contacts.[4]

In electrical measurements the wires connected to the 2DEG sample are usually heat sunk to the coldest part of the cryostat. To achieve the lowest T_e requires strong thermal coupling, achieved by minimizing the contact resistance R_C between the 2DEG and the ohmic contact. We have achieved this using 4mm×4mm samples, see schematic in Fig. 1(a) inset, and elsewhere we have used one of these samples to demonstrate[5] an electron temperature of $T_e = 1$ mK, with a heat leak to the 2DEG in the fW range. In this Letter we report the unexpected discovery that the AuNiGe contacts become superconducting below 1 K. The superconductivity in the ohmic contact appears as a variable series resistance to the 2DEG sample, and will hinder how the electrons in the 2DEG are cooled to ultra-low temperatures.

Results are presented from three wafers, W476, V827 and V834, which have the same structure and were grown in two different molecular beam epitaxy machines (V & W). The 2DEG is created 90 nm below the sample surface at the $Al_{0.33}Ga_{0.67}As$/GaAs interface; on top of the undoped GaAs there is 80 nm of $Al_{0.33}Ga_{0.67}As$, capped with a 10 nm GaAs top layer. There is Si-doping in the upper 40 nm of AlGaAs, giving a spacer layer distance of 40 nm between the dopants and the 2DEG. After illumination with a red light-emitting diode (LED) the 2DEGs have a mobility at 4.2 K of $\mu \approx 2 \times 10^6$ cm^2/Vs at $n_{2D} \approx 3 \times 10^{11}$ cm^{-2}. The corresponding sheet resistance is $R_{sh} \approx 10\ \Omega/\square$.

Since their discovery[6] in 1967, alloys of Au, Ni, and Ge have been routinely used to make ohmic contact to electrons in GaAs-based devices. A summary of the history, mechanism and morphology of these contacts is given in Ref. 7, and references therein. Many factors influence the contact resistance to a 2DEG: the depth of the 2DEG; the thickness of the AlGaAs layer; the sequence, thickness and composition of the contact metal layers; the target temperature of the rapid thermal annealer; the annealing time; the mobility of the 2DEG; and the quality of the sample surface before deposition. Low normalized contact resistances $r_c \sim 0.05$ Ωmm have been demonstrated[8] in 2DEGs with mobilities of $\sim 10^5$ cm^2/Vs; using similar recipes we have obtained $r_c \sim 1$ Ωmm in higher mobility 2DEGs.

Results from six samples (A-F) from four different processing batches (I-IV) are presented here. Sample A was fabri-

[a)] Electronic mail: james.nicholls@rhul.ac.uk

cated by thermally evaporating 160 nm of AuNiGe from a eutectic slug (by weight: 83% Au, 5% Ni, 12% Ge). Sample B was fabricated by evaporating 3 nm Ni, then 136 nm eutectic AuGe (by weight: 88% Au, 12% Ge), then a further 30 nm of Ni, which is capped by 180 nm of Au. The layer sequences for the other samples are summarized in Table I. All contacts were annealed in a forming gas (N_2 + H_2) at 430°C in a rapid thermal annealer for 80 s. These annealing conditions give the lowest R_C, in agreement with the U-shaped dependence of the contact resistance on annealing temperature.[7,9]

TABLE I. Processing conditions of samples A-F.

Sample (wafer)	Processing conditions (batch name)
A (W476)	160 nm eutectic AuNiGe (I)
B (V827)	3 nm Ni, 136 nm AuGe, 30 nm Ni, 180 nm Au (II)
C (V834)	130 nm AuGe, 50 nm, 164 nm Au (III)
D (V834)	123 nm AuGe, 30 nm Ni, 200 nm Au (IV)
E (V834)	3 nm Ni, 136 nm AuGe, 30 nm Ni, 180 nm Au (II)
F (V834)	3 nm Ni, 136 nm AuGe, 30 nm Ni, 180 nm Au (II)

To minimize the contact resistance R_C and hence improve the cooling of electrons in the 2DEG, we have fabricated samples with large ohmic contacts. The Fig. 1(a) inset shows a schematic of the 4mm×4mm sample, which consists of two 4mm×1mm current contacts (I^+, I^-) on either side of a 4mm×2mm 2DEG. There are three 200μm×200μm contacts: two voltage probes (V^+, V^-) on one side of the sample, and a third one (unused) on the opposite side.

To determine the contact resistance R_C of the current contacts, we compare four-terminal (4T) and two-terminal (2T) resistance measurements. The circuit in the Fig. 1(a) inset shows an AC current driven between I^+ and I^-, a voltage is either measured (V_{4T}) between the two voltage contacts (V^+,V^-), or between (V_{2T}) the current contacts using extra gold bond wires. The region of 2DEG of length 1.2 mm and width 4 mm has a 4T resistance $R_{4T} = V_{4T}/I = \frac{1.2}{4} R_{sh} = 0.3\,R_{sh}$. If the R_C of the I^+ and I^- contacts are equal, then the 2T resistance of the whole 2DEG, of length 2 mm and width 4 mm, is

$$R_{2T} = 2R_C + R_{2DEG} = 2R_C + \frac{2}{4} R_{sh} = 2R_C + \frac{5}{3} R_{4T}. \quad (1)$$

4T and 2T measurements between different pairs of contacts show that the 2DEG is homogeneous and that the R_C for similar contacts are equal, both before and after illumination with a red LED; we show results after illumination.

Resistance measurements were performed on a dilution fridge, where the samples sit in vacuum inside a superconducting magnet with the field B applied perpendicular to the 2DEG. The copper wires providing electrical connections to the sample, mounted in a ceramic chip carrier, are wound around copper heating-sinking posts that are firmly bolted to the mixing chamber plate of the dilution fridge. Figure 1(a) shows $R_{2T}(B)$ measurements of sample A at $T = 0.03$ K. At zero field, $R_{2T} \sim 5\,\Omega$, but with increasing B-field a linear magnetoresistance due to the Hall effect dominates, as has been observed[10] in $R_{2T}(B)$ measurements of graphene. In both

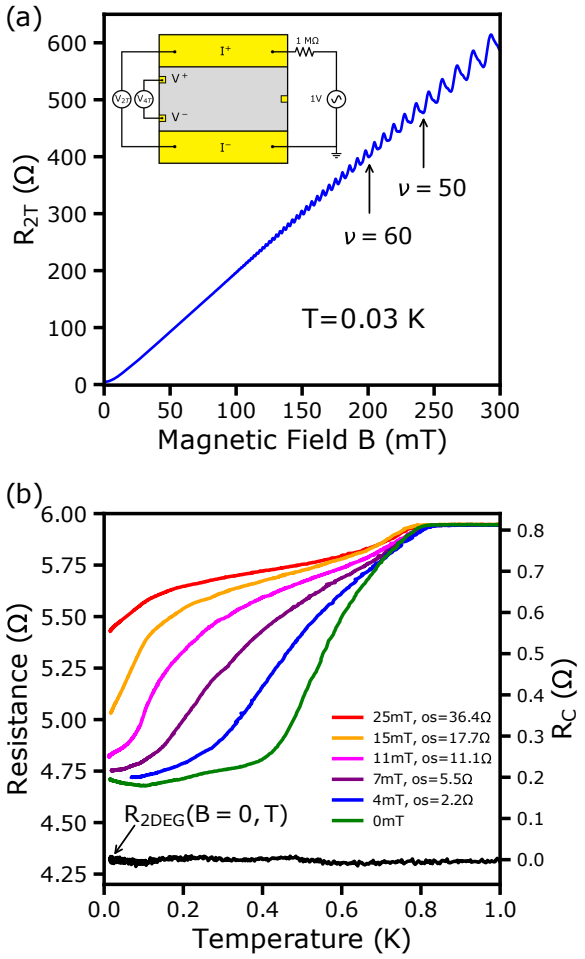

FIG. 1. Sample A. (a) $R_{2T}(B)$ measurement at $T = 0.03$ K. For $B > 0.1$ T, Shubnikov-de Haas oscillations in R_{xx} become visible, and the Landau level filling factors are indexed for $\nu = 50$ and 60. Inset: Schematic of the 4mm×4mm device. The four-terminal resistance of the 2DEG between V^+ and V^- is given by $R_{4T} = V_{4T}/I$, when an AC current $I = 1$ μA is passed between I^+ and I^-. The corresponding 2T resistance between I^+ and I^- is $R_{2T} = V_{2T}/I$. (b) Traces of $R_{2T}(T)$ at $B = 0, 4, 7, 11, 15$, and 25 mT. The sweeps at finite B have been shifted down by the given offsets (os) to remove the magnetoresistance of the 2DEG. $R_{2DEG}(T) = 4.32\,\Omega$ at $B = 0$ is the trace shown in black. The contact resistance, $R_C = (R_{2T} - R_{2DEG})/2$, is given on the right hand y-axis.

cases the current contacts span the whole width of the sample, shorting the Hall voltage between them, so that even at low fields it is much larger than the voltage across the longitudinal resistance R_{xx}. Theoretically[11] the two-terminal resistance is $R_{2T}(B) = c\sqrt{R_{xx}^2 + R_{xy}^2}$, where $R_{xy} = \frac{B}{n_{2D}\,e}$ is the Hall resistance, and the prefactor c is of order unity. With increasing B, $R_{xy} \gg R_{xx}$, $c \to 1$, and $R_{2T} \to R_{xy}$. The linear $R_{2T}(B)$ below 0.1 T has a gradient of 2050 ΩT^{-1}, which corresponds to $n_{2D} = 3.04 \times 10^{11}$ cm^{-2}, consistent with $n_{2D} = 2.94 \times 10^{11}$ cm^{-2} obtained from the indexed Shubnikov-de Haas oscillations in $R_{xx}(B)$.

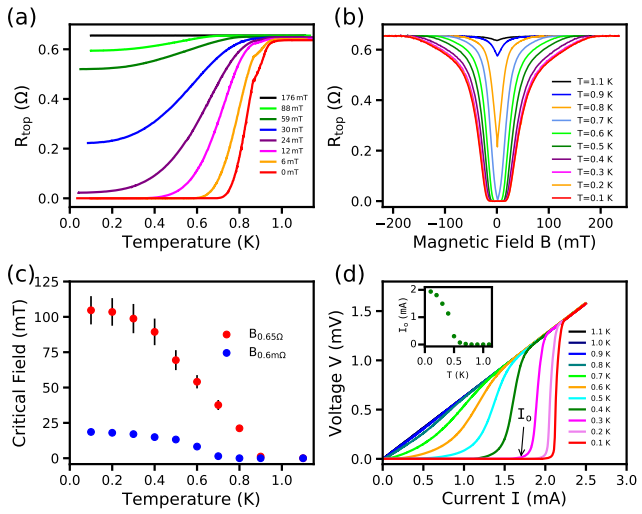

FIG. 2. Sample B: (a) $R_{\rm top}(T)$ traces when cooled in constant B fields up to 176 mT. (b) $R_{\rm top}(B)$ sweeps at constant temperatures between 0.1 K and 1.1 K. (c) "Critical fields" of the superconductor: $B_{6{\rm m}\Omega}$ is the field where $R_{\rm top} = 6$ mΩ, and $B_{0.65\Omega}$ when $R_{\rm top}$ first reaches 0.65 Ω. (d) V-I characteristics at different constant temperatures. The onset current $I_{\rm o}$ is indicated with an arrow for the sweep at 0.3 K. Inset: $I_{\rm o}$ plotted for different temperatures.

Figure 1(b) shows the two-terminal resistance $R_{2{\rm T}}(T)$ of the same sample. At $B = 0$, $R_{2{\rm T}}(T)$ shows a 1.2 Ω drop in resistance below 0.8 K, which has contributions (see Eq. 1) from $R_{\rm C}$ and $R_{2{\rm DEG}}$. The $R_{2{\rm T}}(T)$ traces at finite B field in Fig. 1(b) are vertically offset to align the resistances at 5.95 Ω for $T > 0.8$ K. The 2DEG resistance at zero field $R_{2{\rm DEG}}(T) = 4.32$ Ω, and when subtracted from the colored $R_{2{\rm T}}(T,B)$ traces gives the quantity $2 \times R_{\rm C}(T,B)$. The right hand y-axis shows $R_{\rm C}$ calculated from Eq. 1: in zero field $R_{\rm C} = 0.8$ Ω for $T \approx 1$ K, dropping to 0.2 Ω at low temperatures. The drop in the contact resistance below 0.9 K is due to the presence of a superconductor in the ohmic contact; with increasing perpendicular magnetic field the superconductivity is suppressed, decreasing the drop in $R_{\rm C}$.

Clearer evidence of superconducting behavior, with a clear drop to a low temperature zero-resistance state, is obtained from surface resistance measurements of a single ohmic contact presented in Figs. 2(a) and (b). $R_{\rm top}$ is a four-terminal measurement of approximately two squares of contact, and Fig. 2(a) shows that at $B = 0$ the resistance drops sharply from $R_{\rm top} = 0.65$ Ω to zero, with the superconducting transition centered at $T_c = 0.83$ K. As B increases, this resistance drop shifts to lower temperature and the low T resistance increases. Eventually at $B = 0.15$ T, $R_{\rm top}$ remains constant as a function of temperature. $R_{\rm top}(B)$ sweeps at constant temperature are shown in Fig. 2(b), and to characterize the superconductor we define two critical fields: when $R_{\rm top}$ reaches 6 mΩ defines $B_{6{\rm m}\Omega}$, and when $R_{\rm top}$ first reaches 0.65 Ω defines $B_{0.65\Omega}$. The two quantities are plotted as a function of temperature in Fig. 2(c); the resulting phase diagram quantifies the effect of B, and is not an indication of whether the superconductor is type I or II.

The superconductivity is also evident in the four-terminal V-I characteristics, see Fig. 2(d), along the top of the same contact. The DC voltage across the top of the contact is measured as the DC current I is swept at a rate of 10 mA/hour. There is hysteresis in the up-down characteristics and only up-sweeps are shown in Fig. 2(d). As a measure of the superconducting behavior we define an onset current $I_{\rm o}$ where the voltage becomes finite, see sweep at 0.3 K. The $I_{\rm o}$ values obtained for different temperatures are plotted in the inset to Fig. 2(d). $I_{\rm o}$ goes to zero at 0.6 K, but the V-I characteristics show non-linear behavior up to $T_c = 0.9$ K.

The $R_{\rm top}$ measurements in Figs. 2 (a) and (b) suggest that there is a superconductor in parallel with a normal layer with a resistance of 0.65 Ω; this latter layer is probably a disordered gold-rich layer with roughly constant resistance even when the magnetic field ($B < 0.15$ T) and temperature ($T < 1.2$ K) are varied. This shunting layer complicates a possible measurement of the superconducting gap, though the data in Fig. 2(d) shows that the V-I characteristics become ohmic as the temperature is increased above 0.9 K. Due to the inhomogeneous structure of the AuNiGe contact, see Fig. 4, it is likely that there is not a uniform layer of superconductor, but a granular superconductor, where there are superconducting grains in close proximity to each other, linking up to form a superconducting path between the gold wire bonds on the contact surface.

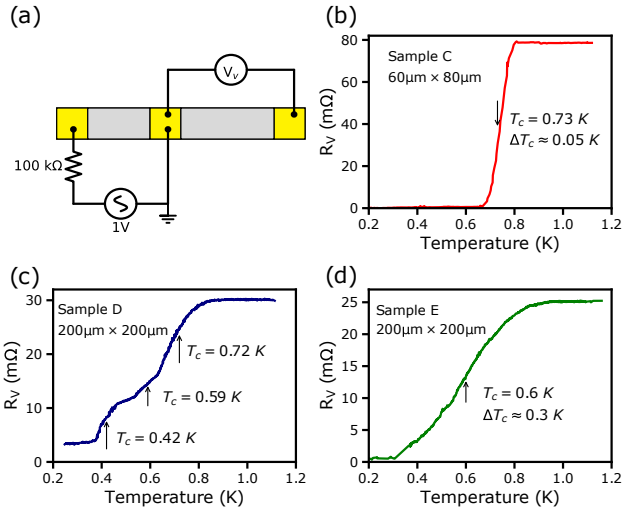

FIG. 3. (a) Circuit used to perform[12] a vertical resistance R_V measurement. $R_V(T)$ sweeps for samples C, D, and E, fabricated from wafer V834: (b) shows a single transition with half-width $\Delta T_c = 0.05$ K, (c) shows evidence of four phases, and (d), shows a broad superconducting transition.

A greater understanding of current-crowding and the modification of the 2DEG sheet resistance R_{sk} *under* the ohmic contact can be obtained[12] from a vertical resistance R_V measurement. Figure 3(a) shows the circuit[12] used to measure $R_V(T)$ in a sample fabricated for conventional transmission line model (TLM) measurements.[13] Results are presented in Figs. 3(b)-(d) for three samples C-E respectively: (b) shows a

narrow superconducting transition at $T_c = 0.73$ K, where for $T < T_c$, $R_V \sim 0.1$ mΩ, which is an approximate measure of the resistance of the Ge-doped semiconductor above the 2DEG. In (c) there is evidence of a least four different phases (three of which are superconducting), and in (d) the superconducting transition is broad, $\Delta T_c \approx 0.3$ K, centered at $T_c = 0.6$ K.

From the study of R_C, R_{top} and R_V in many samples, there are a number of important trends which we summarize below:
(i) The broadest transitions were obtained with AuNiGe eutectic contacts (batch I), and the narrowest transitions with the highest T_c were generally obtained in batches II and III. Otherwise, it is difficult to correlate the different superconducting phases observed with the processing conditions.
(ii) Both T_c and the drop in resistance R_C, R_{top} and R_V below T_c, are similar before and after illumination with an LED. This reinforces the picture that the superconductor lies in the material *above* the 2DEG, and is in series with the 2DEG.
(iii) For $T > T_c$, both R_{top} and R_V are constant up to $T \sim 20$ K, behavior characteristic of a disordered alloy.
(iv) For a typical 200μm×200μm contact: R_C =2-3 Ω and R_V = 25-30 mΩ for $T > T_c$. Using the current-crowding model[12] the transfer length is $T_L \approx 40$ μm and the resistance of the 2DEG *under* the contact is $R_{sk} \approx 16$ Ω/□, greater than the sheet resistance in the bulk 2DEG. How the current-crowding model is modified by the superconductivity is beyond the scope of this paper.

Figure 4 shows a cross-sectional scanning electron microscope (SEM) image taken of a current contact in a 4mm×4mm device. The inhomogeneous microstructure within the top metal layer of the contact is consistent with previous studies.[7,14,15] The top is Au-rich and there are Ni- and As-rich inclusions positioned just above the interface with the GaAs. The inclusions are typically 0.1-0.5 μm in size and are well spaced apart, although the one large inclusion on the right protrudes through to the surface of the ohmic contact. The waviness of the interface with the GaAs suggests that some of the semiconductor has been consumed during annealing.

Structural studies[7] show that Ge forms compounds with Ni and As, prior to diffusing into the GaAs as the *n*-type dopant, displacing the Ga which then diffuses into the upper part of the contact - this is the large continuous region labelled Au-Ga matrix in the SEM image in Fig. 4. The most commonly observed[14–20] Au-Ga alloy in AuNiGe contacts is β-AuGa, but it is not known to be superconducting. However, there are other gallium-based superconductors with a $T_c \sim 1$ K which could be present in the matrix:
• α-AuGa: Ga dissolves into Au to form $Au_{1-x}Ga_x$. T_c ranges[21] from 8 mK to 264 mK, as x varies from 0.03 to 0.1.
• AuGa has a $T_c = 1.1$ K and $B_c = 5.7$ mT.[22]
• $AuGa_2$ has a $T_c = 1.63$ K and $B_c \gg 10$ mT.[22]
• α-Ga: $T_c = 0.9$ K and a critical field of 5.8 mT.
α-AuGa has been observed[16] in contacts annealed at 600°C, but if the contacts are annealed at 450°C they only contain β-AuGa. There is little evidence in the literature of the other three superconductors being present. Table S3 of the SI lists many of the compounds and elements that have been identified in AuNiGe contacts, together with other superconductors that could be formed from AuNiGe and GaAs/AlGaAs. Without a full structural study it is not possible to identify the superconductor(s) in the AuNiGe contacts.

In conclusion, we have shown that low resistance ohmic contacts to high mobility GaAs-based 2DEGs can be fabricated by annealing either AuNiGe eutectic or AuGe eutectic/Ni layers at 430°C. A typical normalized contact resistance is at best $r_c \sim 1$ Ωmm, and for the 4mm×4mm devices the contact resistance is $R_c \sim 1$ Ω. An unexpected result is that the ohmic contact becomes superconducting causing the contact resistance to drop by roughly 0.5 Ω; we report transitions with $T_c \leq 0.9$ K and saturation of the resistance in a perpendicular magnetic field of $B_c = 0.15$ T. Changes in the contact resistances will not affect four-terminal measurements of a 2DEG, and will be hard to detect in two-terminal conductance measurements which are usually performed on high resistance ($\gg 1$ kΩ) samples. We show that the clearest and most straightforward characterization of the T_c and B_c of the superconductor comes from measurements of the surface resistance R_{top} of one of the ohmics. The resistance measurement of R_V is particularly sensitive to vertical transport; the normal state resistance allows a determination of the transfer length, and the low temperature zero-resistance state suggests a three-dimensional superconducting network.

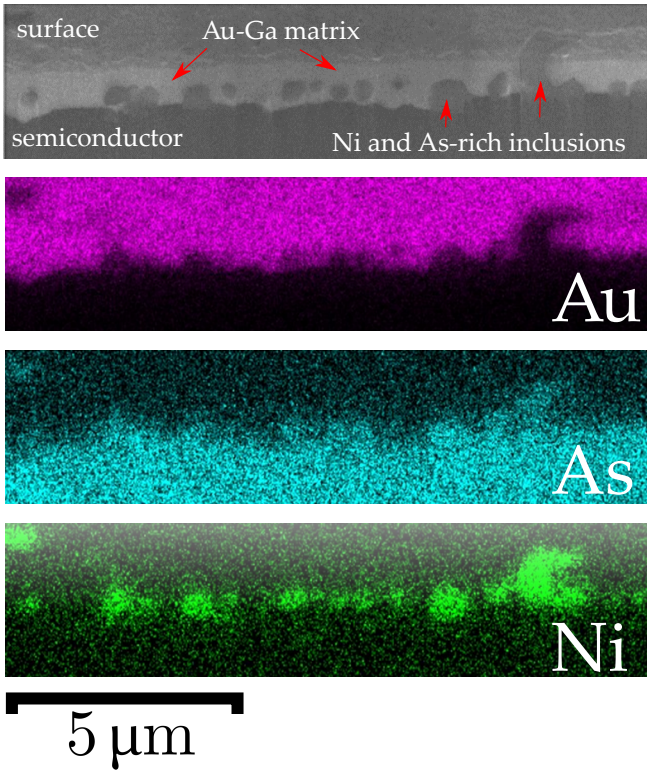

FIG. 4. Sample F: scanning electron micrograph (SEM) of the sidewall of a trench cut into a current contact using a Ga focussed ion beam. The light material just below the surface is Au-rich, within it and near the semiconductor interface are dark Ni-rich inclusions that are 0.1-0.5 μm in size. The energy dispersive x-ray (EDX) maps show that the inclusions contain no Au, but have high concentrations of Ni and As.

Although the R_c of the contacts are lower below T_c, the overriding effect will be their reduced ability to cool the 2DEG because superconductors have low thermal conductivities.[23] Using noise thermometry on a 4mm×4mm similar to sample A, where the electrons are cooled in a ^{3}He immersion cell, Levitin *et al.*[5] report that at 1-3 mK the thermal conductance through the contacts is about 10% of that expected from applying the Wiedemann-Franz law to their normal state electrical resistances $R_C \approx 1\ \Omega$. Given the widespread use of AuNiGe contacts annealed at 400-450°C for both GaAs- and InGaAs-based 2DEGs, it is possible superconducting contacts were used in previous studies and the superconductivity in low magnetic fields (< 0.15 T) could be the factor why it has been historically difficult to cool GaAs-based 2DEGs below 50 mK until recently. An alternative would be to use ohmic contacts made with gold-free recipes, for example PdGe contacts,[24] as the Pd-Ga alloys are not known to be superconducting.

SUPPLEMENTARY MATERIAL

See supplementary material for further information on the measurement circuits, the wafer structure, processing conditions, microstructure, as well as resistance measurements in a parallel magnetic field. There is also a table of possible superconductors that can be generated from the elements within the samples.

ACKNOWLEDGMENTS

This work was supported by EPSRC (UK) Programme grant EP/K004077, and by EU H2020 European Microkelvin Platform EMP, Grant No. 824109. The authors thank E. W. Tapley for technical assistance. J.W. acknowledges funding from the Herchel Smith Fund at the University of Cambridge.

Data availability: The data that support the findings of this study are available from the corresponding author upon reasonable request.

[1] Z. Iftikhar, A. Anthore, S. Jezouin, F. D. Parmentier, Y. Jin, A. Cavanna, A. Ouerghi, U. Gennser, and F. Pierre, Nature Communications **7**, 12980 (2016).
[2] A. Anthore, Z. Iftikhar, E. Boulat, F. D. Parmentier, A. Cavanna, A. Ouerghi, U. Gennser, and F. Pierre, Phys. Rev. X **8**, 031075 (2018).
[3] Z. Iftikhar, A. Anthore, A. K. Mitchell, F. D. Parmentier, U. Gennser, A. Ouerghi, A. Cavanna, C. Mora, P. Simon, and F. Pierre, Science **360**, 1315–1320 (2018).
[4] N. J. Appleyard, J. T. Nicholls, M. Y. Simmons, W. R. Tribe, and M. Pepper, Phys. Rev. Lett. **81**, 3491 (1998).
[5] L. V. Levitin, H. van der Vliet, T. Theisen, S. Dimitriadis, M. Lucas, A. D. Corcoles, J. Nyeki, A. J. Casey, G. Creeth, I. Farrer, D. A. Ritchie, J. T. Nicholls, and J. Saunders, "Preprint: Cooling low-dimensional electron systems into the microkelvin regime," (2020).
[6] N. Braslau, J. B. Gunn, and J. L. Staples, Solid State Electron. **10**, 381 (1967).
[7] M. Murakami, Science and Technology of Advanced Materials **3**, 1 (2002).
[8] T. S. Abhilash, C. R. Kumar, and G. Rajaram, Journal of Physics D: Applied Physics **42**, 125104 (2009).
[9] A. Christou and N. Papanicolaou, Solid-State Electronics **29**, 189 (1986).
[10] J. R. Williams, D. A. Abanin, L. DiCarlo, L. S. Levitov, and C. M. Marcus, Physical Review B **80**, 045408 (2009).
[11] D. A. Abanin and L. S. Levitov, Physical Review B **78**, 035416 (2008).
[12] G. K. Reeves and H. B. Harrison, IEEE Electron Device Letters **3**, 111 (1982).
[13] H. H. Berger, Solid-State Electronics **15**, 145 (1972).
[14] Y.-C. Shih, M. Murakami, E. L. Wilkie, and A. C. Callegari, Journal of Applied Physics **62**, 582 (1987).
[15] H. Goronkin, S. Tehrani, T. Remmel, P. L. Fejes, and K. J. Johnston, IEEE Transactions on Electron Devices **36**, 281 (1989).
[16] M. Murakami, K. D. Childs, J. M. Baker, and A. Callegari, Journal of Vacuum Science & Technology B: Microelectronics Processing and Phenomena **4**, 903 (1986).
[17] A. Baranska, A. Szerling, P. Karbownik, K. Hejduk, M. Bugajski, A. Laszcz, K. Golaszewska-Malec, and W. Filipowski, Optica Applicata **43**, 5 (2013).
[18] R. K. Ball, Thin Solid Films **176**, 55 (1989).
[19] A. K. Rai, R. S. Bhattacharya, and Y. S. Park, Thin Solid Films **114**, 379 (1984).
[20] A. J. Barcz, E. Kaminska, and A. Piotrowska, Thin Solid Films **149**, 251 (1987).
[21] R. Hoyt and A. Mota, Solid State Communications **18**, 139 (1976).
[22] R. A. Hein, J. E. Cox, J. Willis, H. R. Khan, and C. J. Raub, Journal of the Less-Common Metals **62**, 197 (1978).
[23] F. Pobell, *Matter and Methods at Low Temperatures* (Springer-Verlag, 2007).
[24] N. K. Patel, J. H. Burroughes, M. J. Tribble, E. H. Linfield, A. C. Churchill, D. A. Ritchie, and G. A. C. Jones, Applied Physics Letters **65**, 851 (1994).